PERFORMANCE EVALUATION OF A PARABOLIC TROUGH COLLECTOR USING OIL-BASED GREEN-SYNTHESIZED NANOFLUIDS

Eric C. Okonkwo[1]*, Edidiong A. Essien[2], Muhammad Abid[1], Doga Kavaz[2], Tahir A.H. Ratlamwala[3]
[1]Department of Energy Systems Engineering, Cyprus International University, North Cyprus, Turkey.
[2]Environmental Research Centre, Cyprus International University, North Cyprus, Turkey.
[3]National University of Sciences and Technology, Islamabad, Pakistan.
Corresponding author: Eric C. Okonkwo, e-mail: echekwube@ciu.edu.tr

REFERENCE NO

SOLR-01

Keywords: PTC; thermal enhancement; green-synthesis; OLE; nanofluid.

ABSTRACT

Performance evaluation of a parabolic trough collector (PTC) using green synthesized nanofluids is performed. The study employed experimental synthesis and numerical modeling to present some possible solution to the challenges of nanofluid application in solar collectors. Two nanoparticles synthesized from olive leaf extract (OLE) are characterized using analytical and morphological techniques and was found to be efficient corrosion inhibitor, non-toxic and cheap to produce. The system is modeled after the LS-2 collector. The results of the analysis show that both nanofluids obtained a better thermal performance than that of the thermal oil. A mean enhancement 0.51% and 0.48% in the thermal efficiency is observed with the use of Syltherm-800/OLE-nZVI and Syltherm-800/OLE-TiO_2 nanofluids respectively. The heat transfer performance of the nanofluids also showed great performance as a mean enhancement of 42.9% and 51.2% is observed with the use of Syltherm-800/OLE-TiO_2 and Syltherm-800/OLE-nZVI nanofluids respectively.

1. INTRODUCTION

The parabolic trough collector (PTC) is a solar concentrating collector characterized with temperature applications ranging from 50-400°C [1]. The collector is made up of a reflective sheet (mirror) bent in a parabola shape and a receiver tube placed at a focal length from the reflective sheet. The reflective sheet (mirror) intercept incident radiation from the sun and focuses it on the receiver tube which is placed at the centre. Fig. 1 gives a diagrammatic representation of this process. The receiver tube has a heat transfer fluid (HTF) flowing through it by which it transfers the concentrated solar radiation by way of convective heat transfer to the fluid. The fluid carries the useful energy to the various applications where it is used. Some of these applications range from electricity production [2], space heating [3], absorption refrigeration systems [4] and other heat powered industrial applications.

The dispersion of nanoparticles into the base fluid used in the PTC has been suggested by many researchers [5, 6]. Most of the results obtained from the literature show that the nanoparticle improved the heat transfer characteristic of the base fluids. Though literature has provided some interesting results with the use of nanofluids in the solar collectors, its application has suffered many limitations. Some of these limitations include sedimentation, corrosion of components, and the high cost of preparation, the toxicity of the nanoparticle, pressure drop and additional pumping power [7, 8].

This study presents some possible solution to the challenges of nanofluids application in solar collectors. It proposes the use of green synthesized nanoparticle from bio-matter: olive leaf extracts (OLE). It presents a novel performance evaluation of a PTC using Syltherm-800 base nanofluids. The nanoparticles were synthesized from olive leaf extract (OLE): OLE-nZVI and OLE-TiO_2 and were tested to be efficient corrosion inhibitor, non-toxic and cheap to produce when compared to the conventional ones. The key parameters to be examined include the thermal efficiency, exergetic efficiency, heat

transfer coefficient inside the tube and pressure drops in the PTC.

The thermal model is based on a detailed heat transfer model presented in [9] which was validated using the experimental results of Dudley [10] AZTRAK platform LS-2 test.

The PTC is modeled after the LS-2 parabolic trough collector and the dimensions are presented in Table 1. The receiver tube is made of stainless steel coated with cermet to increase its absorptivity to incoming radiation. The stainless steel tube is enveloped in a glass cover to reduce convective heat losses. The space between the glass cover and the receiver is evacuated at a pressure as low as 0.0103 Pa [11].

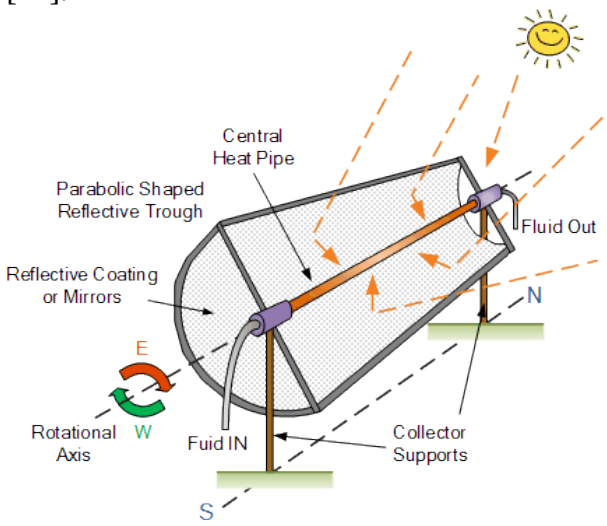

Fig. 1. Parabolic trough collector system

Table 1. Characteristics of the LS-2 parabolic solar collector.

Parameter	Value
Aperture area	39.2m^2
Focal length	1.84m
Peak optical efficiency	75.5%
Absorber tuber diameter inner/outer	66mm/70mm
Glass cover diameter inner/outer	109mm/115mm
Concentration ratio	22.74
Emittance of glass cover	0.86

1.1. Nanoparticles preparation

The nanoparticles (NP) used in this study are the zero valent iron nanoparticle (nZVI) and the titanium dioxide nanoparticle (TiO_2). These nanoparticles were synthesized from olive leaf extract (OLE) and Fig. 2 describes the process.

Fresh Olive leaves were collected from Cyprus International University farm. They were washed convincingly in distilled water, dried in an oven at 40°C for 24 hours and crushed with an electric blender. 10g of the crushed OLE was extracted in ethanol, concentrated using a rotary evaporator, filtered and then stored in a refrigerator. For the titanium dioxide nanoparticle 80mL of 1.0M titanium (IV) chloride was mixed with 20 mL of the freshly prepared OLE in Erlenmeyer flask and stirred with homogenization stirrer at 4000rpm for 1 hour at room temperature. Colour change was observed visually and also using JASCO 670 UV/Vis spectrophotometer.

During the synthesis of zero valent iron NPs, both the precursor and the reducing agent were mixed in a nitrogen environment. For the reduction of Iron (III) chloride, 20ml of filtered OLE was mixed to 10ml of freshly prepared 0.001M aqueous $FeCl_3.6H_2O$ solution. The solution was added drop-by-drop. Colour change was observed visually and also using JASCO 670 UV/Vis spectrophotometer.

The particle size of both nanoparticles in the composite was determined using particle sizer. JASCO 670 UV/Vis spectrophotometer was used for UV–Vis analyses [12]. For X-ray diffraction (XRD) analysis, the nanoparticles developed were centrifuged at 6000rpm for 30mins. The settling solid residues were washed twice with double distilled water and then re-dissolved in absolute ethanol and evaporated to dryness at 80^{o}C to obtain powdered nanoparticles. Also, the morphology of the nanoparticles was observed using SEM J Quanta FEG 250 model (FEI, Holland). The thermogravimetric analysis (TGA) and differential scanning calorimetry were investigated using (SDT Q600 TA instrument) to check the residual weight and thermal degradation of the OLE-TiO_2-NP. Thermal conductivity test was performed using the KD2 Prothermal properties analyzer (Decagon, USA). The prepared sample was then analyzed using a single point thermal method for the examination. The density of the nanoparticle was determined by using a

DA 130 density meter (Kyoto Electronics, Japan). A DSC 4000 differential scanning calorimeter (Perkin Elmer, USA) was used to determine the specific heat of the Titanium dioxide nanoparticles. These analyses were conducted at two different temperatures (300K and 400K).

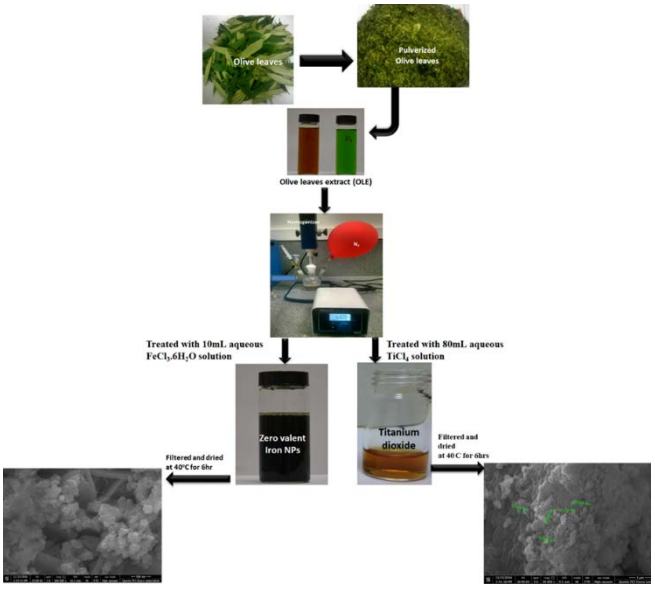

Fig. 2. Pictorial representation of nanoparticle preparation

Table 2. Thermophysical properties of the nanoparticles.

Parameters	**Nanoparticles**	
	OLE-nZVI	***OLE-TiO_2***
Specific heat capacity (J/kg.k)	670	2406
Thermal Conductivity (W/m.k)	7.10	0.780
Density (Kg/m^3)	3560	1120
Particle size (nm)	70	70

2. MATHEMATICAL MODELING

The detailed equations for the energy balance, thermal and exergetic model can be found in references [1]. The system is modeled using the engineering equation solver (EES) under steady-state conditions.

2.1. Energy and Exergy Analysis

The model for the thermal analysis of the PTC is presented here, the available solar radiation, thermal efficiencies, and useful energy are all necessary parameters for solar system's validation.

The energy balance equation is the key parameter used in obtaining the useful energy in the system and is presented as:

$$Q_u = \dot{m} \cdot C_p \cdot (T_{out} - T_{in}) \quad (1)$$

The amount of solar radiation from the sun incident on the collector is obtained using equation (1).

$$Q_s = A_a \cdot G_b \quad (2)$$

The thermal efficiency can thus be calculated as

$$\eta_{th} = \frac{Q_u}{Q_s} \quad (3)$$

The exergy output of the collector is given as

$$E_u = Q_u - \dot{m} \cdot C_p \cdot T_{amb} \cdot \ln\left(\frac{T_{out}}{T_{in}}\right) \quad (4)$$

The exergy of the sun is given by Petela, [13] as

$$E_s = A_c \cdot G_b \cdot [1 - \frac{4}{3} \cdot \left(\frac{T_{amb}}{T_s}\right) + \frac{1}{3} \cdot \left(\frac{T_{amb}}{T_s}\right)^4 \quad (5)$$

where, T_s is 5800K and it represents the apparent temperature of the sun as a black body [13]. The exergy efficiency represents the maximum possible useful work that could be extracted from a system and is presented as

$$\eta_{ex} = \frac{E_u}{E_s} \quad (6)$$

2.2. Nanofluids

Two different nanofluids are used in this study. The Syltherm-800/ OLE-TiO_2 nanofluid and the Syltherm-800/ OLE-nZVI nanofluid. The properties of the nanoparticles are outlined in Table 2. From studies related to nanoparticles [7, 14], the density of a nanofluid is obtained using:

$$\rho_{nf} = \rho_{bf}.(1 - \varphi) + \rho_{np}.\varphi \quad (7)$$

The specific heat capacity is obtained using equation (8) from [15].

$$C_{p_{nf}} = \frac{\rho_{bf}.(1-\varphi)}{\rho_{nf}}.C_{p_{bf}} + \frac{\rho_{nf}.\varphi}{\rho_{np}}.C_{p_{np}} \quad (8)$$

The dynamic viscosity is obtained using equation (9) from [16].

$$\mu_{nf} = \mu_{bf}.(1 + 2.5.\varphi + 6.5.\varphi^2) \quad (9)$$

The thermal conductivity is obtained from Bruggeman's model [17]:

$$k_{nf} = 0.25 \cdot [(3\varphi - 1)k_{np} + (2 - 3\varphi)k_{bf} + \sqrt{S}] \quad (10)$$

$$S = [(3\varphi - 1)k_{np} + (2 - 3\varphi)k_{bf}]^2 + 8k_{np} \cdot k_{bf} \quad (11)$$

The volumetric fraction φ of the nanoparticle was used at 3%.

2.3. Heat transfer

Pressurized water is also used as a working fluid in the system. The heat transfer characteristic of the fluid is obtained using the Gnielinski equation [18] for turbulent flow in a tube for 3000 ≤ Re ≤ 5×106 and 0.5 ≤ Pr ≤ 2000 as:

$$N_u = \frac{(\frac{f}{8})\cdot(R_e - 1000)\cdot P_r}{1+12.7\left(\frac{f}{8}\right)^{0.5}(P_r^{\frac{2}{3}}-1)} \quad (12)$$

$$P_r = \frac{\mu \cdot c_p}{k} \quad (13)$$

where Nu is the Nusselt number, Re is the Reynolds number, Pr is the Prandtl number and f is the friction factor. The friction factor can be calculated from the Darcy equation:

$$f = (0.790lnR_{eD} - 1.64)^{-2} \quad (14)$$

Xuan and Li, [19] presented an experimental correlation for obtaining the Nusselt number of a nanofluid. There proposed correlation considers the volumetric fraction φ of the nanoparticle and is given as:

$$N_u = 0.0059 \cdot (1 + 7.628 \cdot \varphi^{0.6886} \cdot P_e^{0.001}) \cdot R_e^{0.9238} \cdot P_r^{0.4} \quad (15)$$

For flows in the turbulent region with Re > 2300 and φ in the range of 0.1% to 2%.

The Reynolds number of the nanofluid is expressed as:

$$R_e = \frac{\rho_{nf} \cdot u \cdot D_{ri}}{\mu_{nf}} \quad (16)$$

The Peclet number of the nanofluid can be calculated from the following equation:

$$P_e = \frac{u \cdot d_p}{\alpha_{nf}} \quad (17)$$

where dp is the diameter of the nanoparticles. In order to calculate the Peclet number, the thermal diffusivity of the nanofluid (α) is defined as:

$$\alpha_{nf} = \frac{k_{nf}}{Cp_{nf} \cdot \rho_{nf}} \quad (18)$$

The nature of the flow inside the receiver tube is dependent on the mass flow rate which is expressed as:

$$\dot{m} = A_{ri} \cdot \rho \cdot u \quad (19)$$

where u represents the fluid flow velocity inside the receiver tube.

The volumetric flow rate (L/min) is another parameter used in literature and is expressed as:

$$V_f = 60000 \cdot u \cdot A_{ri} \quad (20)$$

3. RESULTS AND DISCUSSION

In this section, the performance of the nanofluids is evaluated against the independent parameters of inlet temperature and volumetric flow rate. The basic simulation parameters used in this study are presented in Table 3.

Table 3. Simulation parameter

Simulation parameters	Values
G_b	900W/m^2
T_{amb}	300K
u_{wind}	1m/s
φ	3%

The thermophysical properties of the nanofluids are presented in Fig. 3 for density and specific heat capacity and in Fig. 4 for viscosity and thermal conductivity. The effect of the nanoparticle dispersion in the Syltherm-800 oil can be seen to greatly improve the properties of density, thermal conductivity, and viscosity of the fluid.

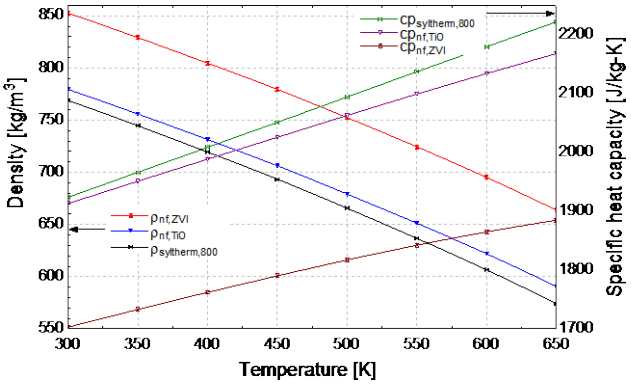

Fig. 3. Comparison of the density and specific heat capacity of the working fluids used

The thermal performance of the working fluid can be seen in Fig. 5. The nanofluids outperform the synthetic oil due to its improved thermo-physical properties.

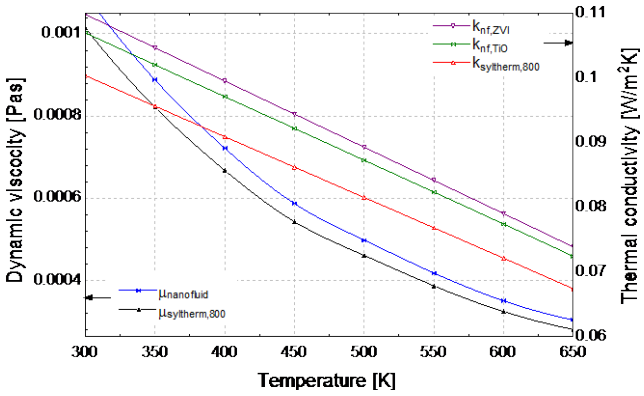

Fig. 4. Comparison of the viscosity and thermal conductivity of the working fluids used

The exergetic efficiency is also seen in Fig. 5 to increase with increasing values of inlet temperature. This is due to the corresponding increase in heat available for useful exergy. The difference in the base fluid and the nanofluids is seen to get greater with higher temperature values.

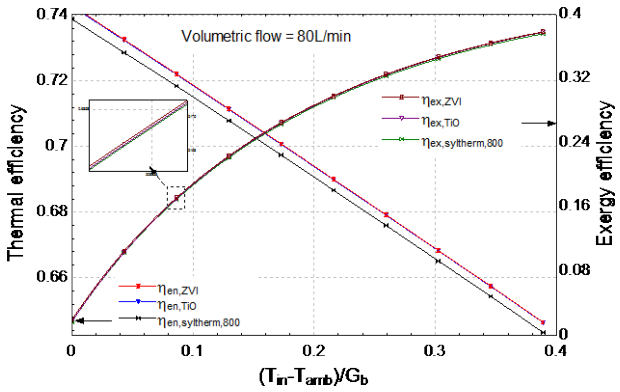

Fig. 5. Thermal and exergetic efficiency comparison for various inlet temperature of the working fluids.

The effect of pressure drop with increase in temperature can be seen in Fig. 6. The nanofluids have a higher pressured drop than the synthetic oil. The difference in pressure drop is seen to decrease with increasing temperature. This decrease is attributed to a decrease in the viscosity levels of the fluid with an increase in temperature.

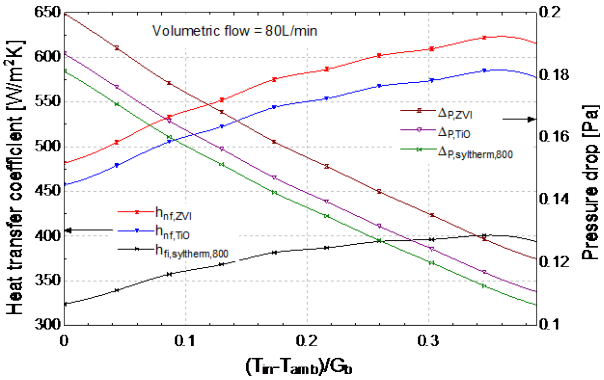

Fig. 6. The effect of inlet temperature on heat transfer coefficient and pressure drop for different working fluids.

The effect of the heat transfer coefficient on varying temperature can also be seen in Fig. 6. The heat transfer coefficient inside the receiver tube is a very important parameter that determines the rate of heat transfer inside the absorber tube. This parameter is influenced by the geometry of the receiver, the properties of the fluid and the mass flow rate of the fluid. The heat transfer coefficient of the nanofluids is at least 40% higher than those of the thermal oil. The value is seen to get greater with higher temperature values.

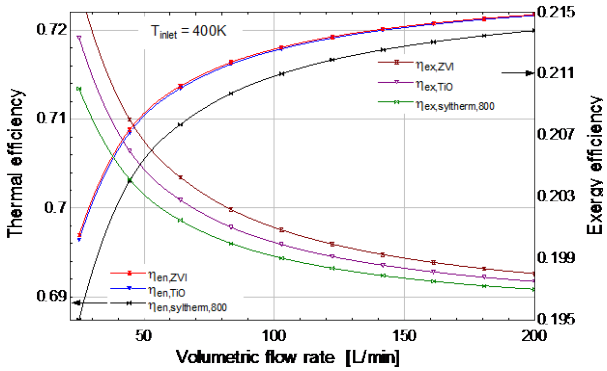

Fig. 7. Thermal and exergetic efficiency of the PTC with an increase in flow rate at a temperature of 400K.

The volumetric flow rate is another independent parameter that affects the mass flow rate, Reynolds number and Nusselt number in the receiver. Varying values of the volumetric flow is investigated for thermal and exergetic efficiencies.

Fig. 7 shows the performance of the thermal and exergetic efficiency against the volumetric flow. The increase in volumetric flow leads to a rise in the thermal efficiency while the opposite is observed with the exergetic efficiency at 400K inlet temperature.

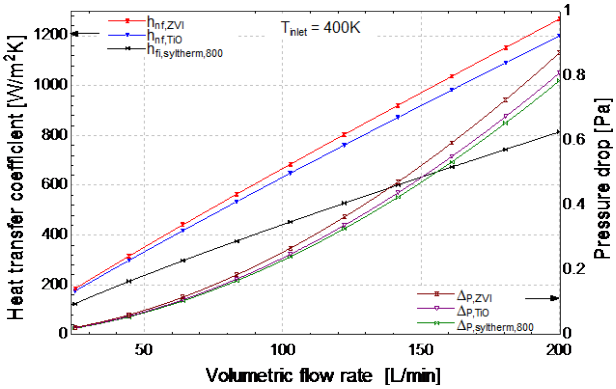

Fig. 8. Heat transfer coefficient and pressure drop of the PTC with an increase in flow rate at a temperature of 400K.

Table 4. Heat transfer coefficient enhancement for all examined fluids at 80l/min.

T_{in}	Sytherm-800 (h_f)	*Enhancements %*	
		Sytherm 800/OLE -nZVI %	*Sytherm-800/ OLE-TiO_2 %*
300	324.3	48.5	41
400	363.2	49.6	41.7
500	387.8	51.7	43.3
550	394.9	53.1	44.3
Mean	**367.5**	**51.2**	**42.9**

The effect of volumetric flow on the heat transfer coefficient and pressure drop is also investigated in Fig. 8. Both values tend to increase with higher numbers of volumetric flow rate. The nanofluids are seen to obtain better heat transfer characteristics as flow rate increases and its difference with the thermal oil gets greater. This is due to the increased level of turbulence in the flow region and thus higher values of Reynolds number. The pressure drop is seen to increase significantly due to the effect of friction of the fluid along the absorber tube.

Table 5. Thermal enhancement for all examined fluids at 80l/min.

T_{in}	Sytherm-800 (η_{th})	*Enhancements %*	
		Sytherm-800/OLE-nZVI %	*Sytherm-800/OLE-TiO_2 %*
300	73.89	0.57	0.53
400	71.24	0.51	0.48
500	68.52	0.48	0.46
550	67.14	0.48	0.45
Mean	**70.19**	**0.51**	**0.48**

From Table 4, it is seen that the nanofluids outperform the base oil with a mean enhancement of 51.2% or the Sytherm 800/OLE-nZVI and 42.9% for the Sytherm 800/OLE-TiO_2. The mean enhancement in thermal efficiencies from Table 5 was observed to be 0.51% and 0.48% for Sytherm 800/OLE-nZVI and Sytherm 800/OLE-TiO_2 respectively.

4. CONCLUSIONS

This study presents a novel performance evaluation of a PTC using Sytherm-800 base nanofluids. The nanoparticles where synthesized from olive leaf extract (OLE): OLE-nZVI and OLE-TiO_2. The study proposes the use of green synthesized nanoparticle from bio-matter to presents some possible solution to the challenges of nanofluids application in solar collectors. The synthesized nanoparticles were characterized using analytical and morphological techniques and was found to be efficient corrosion inhibitor, non-toxic and cheap to produce when compared to the conventional ones. The PTC was modeled after the commercially available LS-2 collector. The model was developed using EES and validated thermally with the experimental data obtained from Dudley [16]. The different combinations of inlet temperature and volumetric flow rates are examined for the nanofluids.

The result of the analysis shows that both nanofluids obtained a better thermal and exergetic performance than that of the thermal oil. A mean enhancement 0.51% and 0.48% in the thermal efficiency is observed with the use of Sytherm-800/OLE-nZVI and Sytherm-800/OLE-TiO_2 nanofluid respectively. The heat transfer performance of the nanofluids also showed incredible performance as a mean enhancement of 42.9% and 51.2% is observed with the use of Sytherm-800/OLE-TiO_2 and Sytherm-800/OLE-nZVI nanofluids respectively. The mean variation in pressure losses between the nanofluids and base fluid was also observed to be less than 11.5% at a nanoparticle volumetric fraction of 3%.

The results shows that the proposed green-synthesized nanofluids has great applications in the PTC especially for higher temperature applications than when compared to the use of thermal oil.

Acknowledgements
The authors acknowledge the support of Corrosion and Electrochemistry Laboratory of the University of Uyo, Nigeria and The Central Laboratory of Duzce University, Turkey.

Nomenclature

A	area (m2)
C_p	specific heat capacity (kJ/kg.K)
D	diameter (m)
d_p	nanoparticle diameter
E	exergy (W)
f	friction factor
G_b	direct normal irradiance (W/m2)
h	heat transfer coefficient (W/m2.K)
K	incident angle modifier
k	thermal conductivity (W/m.K)
L	length (m)
$\dot{m}$	mass flow rate (kg/s)
M	mole
Nu	Nusselt number
P	pressure (KPa)
Pe	Peclet number
Pr	Prandtl number
Q	heat flux (W)
Re	Reynolds number
T	temperature (K)
u	velocity (m/s)
V_f	Volumetric flow rate (L/min)

Greek Letters

ΔP	pressure drop (kPa)
η	efficiency
μ	dynamic viscosity (Pa s)
ρ	density (m3)
φ	volumetric fraction of nanoparticle %
α	Thermal diffusivity

Subscript/ superscript

a	aperture
amb	ambient
bf	base fluid
c	collector
ex	exergetic
f	fluid
fm	mean fluid
g	glass cover
gi	inner glass cover
in	inlet
nf	nanofluids
np	nanoparticles
o	outlet
r	receiver
ri	inner receiver
s	solar/sun
th	thermal
u	useful

Abbreviations

EES	engineering equation solver
$FeCl_3$	Iron (III) chloride
HCl	hydrochloric acid
HTF	Heat transfer fluid
NP	nanoparticle
NREL	National renewable energy laboratory
nZVI	zero valent iron nanoparticle
OLE	olive leaf extract
PTC	Parabolic trough collector
SNL	Sandia national laboratory
$TiCl_4$	Titanium chloride
TiO_2	Titanium dioxide
XRD	X-ray diffraction

References

[1] J. A. Duffie and W. A. Beckman, *Solar Engineering of Thermal Processes Solar Engineering*. John Wiley & Sons, Inc., 2013.

[2] E. C. Okonkwo, C. F. Okwose, and S. Abbasoglu, "Techno-Economic Analysis of the Potential Utilization of a Hybrid PV-Wind Turbine System for Commercial Buildings in Jordan," *Int. J. Renew. Energy Res.*, vol. 7, no. 2, pp. 908–914, 2017.

[3] M. ángel Hernández-Román, A. Manzano-Ramírez, J. Pineda-Piñón, and J. Ortega-Moody, "Exergetic and thermoeconomic analyses of solar air heating processes using a parabolic trough collector," *Entropy*, vol. 16, no. 8, pp. 4612–4625, 2014.

[4] M. Abid, T. A. H. Ratlamwala, and U. Atikol, "Performance assessment of parabolic dish and parabolic trough solar thermal power plant using nanofluids and molten salts," *Int. J. Energy Res.*, vol. 40, pp. 550–563, 2015.

[5] A. J. Chamkha, I. V. Miroshnichenko,

and M. A. Sheremet, “Numerical analysis of unsteady conjugate natural convection of hybrid water-based nanofluid in a semi-circular cavity,” *J. Therm. Sci. Eng. Appl.*, vol. 9, no. December, pp. 1–9, 2017.

[6] R. Loni, E. A. Asli-ardeh, B. Ghobadian, A. B. Kasaeian, and S. Gorjian, “Thermodynamic Analysis of a Solar Dish Receiver using Different Nanofluids,” *Energy*, vol. 133, pp. 749–760, 2017.

[7] A. K. Hussein, “Applications of nanotechnology to improve the performance of solar collectors - Recent advances and overview,” *Renew. Sustain. Energy Rev.*, vol. 62, pp. 767–790, 2016.

[8] D. H. Sukarno, “Challenges for nanofluid applications in heat transfer technology This,” *J. Phys. Conf. Ser.*, vol. 795, no. 1, pp. 3–10, 2017.

[9] E. C. Okonkwo, M. Abid, and T. A. H. Ratlamwala, “Exergetic analysis of a parabolic trough collector with modified absorber geometries using synthetic oil–Al2O3 nanofluid: A comparative study,” Northern Cyprus, 3, 2018.

[10] V. E. Dudley, G. J. Kolb, A. R. Mahoney, T. R. Mancini, C. W. Matthews, M. Sloan, D. Kearney, and Dudley V; Kolb G; Sloan M; Kearney D., “Test results: SEGS LS-2 solar collector,” *Sandia National Laboratories*, vol. 96. p. 11437, 1994.

[11] A. Mwesigye, Z. Huan, and J. P. Meyer, “Thermodynamic optimisation of the performance of a parabolic trough receiver using synthetic oil–Al2O3 nanofluid,” *Appl. Energy*, vol. 156, pp. 398–412, 2015.

[12] M. Sundrarajan and S. Gowri, “Green synthesis of titanium dioxide nanoparticles by nyctanthes arbor-tristis leaves extract,” *Chalcogenide Lett.*, vol. 8, no. 8, pp. 447–451, 2011.

[13] R. Petela, “Exergy of Heat Radiation,” *J. Heat Transfer*, vol. 86, no. 2, p. 187, 1964.

[14] M. Abid, T. A. H. Ratlamwala, and U. Atikol, “Solar assisted multi-generation system using nanofluids: A comparative analysis,” *Int. J. Hydrogen Energy*, vol. 42, no. 33, pp. 21429–21442, 2017.

[15] K. Khanafer and K. Vafai, “A critical synthesis of thermophysical characteristics of nanofluids,” *Int. J. Heat Mass Transf.*, vol. 54, no. 19–20, pp. 4410–4428, 2011.

[16] G. K. Batchelor, “The effect of Brownian motion on the bulk stress in a suspension of spherical particles,” *J. Fluid Mech.*, vol. 83, no. 1, p. 97, 1977.

[17] A. Mwesigye and J. P. Meyer, “Optimal thermal and thermodynamic performance of a solar parabolic trough receiver with different nanofluids and at different concentration ratios,” *Appl. Energy*, vol. 193, pp. 393–413, 2017.

[18] V. Gnielinski, “New equations for heat and mass transfer in turbulent pipe and channel flow.pdf,” *Int. Chem. Eng.*, vol. 16, no. 2, pp. 359–368, 1976.

[19] Y. Xuan and Q. Li, “Investigation on Convective Heat Transfer and Flow Features of Nanofluids,” *J. Heat Transfer*, vol. 125, no. 1, p. 151, 2003.